Stochastic Resonance in the Fermi-Pasta-Ulam Chain

George Miloshevich,[1] Ramaz Khomeriki,[1,2] and Stefano Ruffo[3]
[1]*Physics Department, Tbilisi State University, 0128 Tbilisi, Georgia*
[2]*Max-Planck-Institut fur Physik komplexer Systeme, 01187 Dresden, Germany*
[3]*Dipartimento di Energetica "Sergio Stecco" and CSDC, Università di Firenze, and INFN, via Santa Marta, 3, 50139 Firenze, Italy*
(Received 15 September 2008; published 15 January 2009)

We consider a damped β-Fermi-Pasta-Ulam chain, driven at one boundary subjected to stochastic noise. It is shown that, for a fixed driving amplitude and frequency, increasing the noise intensity, the system's energy resonantly responds to the modulating frequency of the forcing signal. Multiple peaks appear in the signal-to-noise ratio, signaling the phenomenon of stochastic resonance. The presence of multiple peaks is explained by the existence of many stable and metastable states that are found when solving this boundary value problem for a semicontinuum approximation of the model. Stochastic resonance is shown to be generated by transitions between these states.

DOI: 10.1103/PhysRevLett.102.020602 PACS numbers: 05.40.−a, 05.45.−a, 73.43.Lp

Since its theoretical discovery [1,2] and experimental verification [3,4] stochastic resonance has become one of the most widespread topics in many different branches of physics, biophysics, and chemistry (see Ref. [5] for a review). It has a wide variety of applications, e.g., in semiconductors, in neuronal systems, electronic and magnetic systems and, recently, even in quantum physics. All these studies are unified by the common idea to represent a bistable system as particle motion in a double well potential. According to this simplification the system begins to jump from one well to the other, following the periodic forcing, when a resonant noise level is attained. These concepts have wide applications to optical systems. In the ring laser, bistability is due to the left-right propagation symmetry of the system, while in absorptive optical media it is a consequence of the existence of different output powers corresponding to the same input pump intensity [6]. This latter situation has some similarities with the system we discuss in this Letter.

This approach cannot be straightforwardly applied to spatially extended systems, where different stable and metastable excited regimes can coexist, especially when the forcing is applied locally. As discussed in [7], the presence of metastable states does not hinder stochastic resonance. In this Letter, we show that stochastic resonance can be realized for the well-known Fermi-Pasta-Ulam (FPU) chain [8] of anharmonic oscillators. Up to now stochastic resonance in coupled one dimensional systems has been considered only when each element of the chain displays bistable properties [9,10]. In our case, bistability characterizes the whole chain, being originated by the coexistence of different stationary regimes corresponding to a single driving amplitude. This coexistence is also at the basis of the nonlinear bistability effect [11,12] which appears when the chain is harmonically driven at one end with out-band frequency and is due to the presence of breatherlike excitations [13] in the system. As a result, the new type of stochastic resonance we discuss in this Letter should show up in a wide range of systems, from Josephson junction parallel arrays [14,15] to coupled optical waveguides [16] and magnetic thin films [17].

The equations of motion for the β-FPU chain (interparticle potential with quadratic and quartic terms) are

$$\ddot{u}_n = u_{n+1} + u_{n-1} - 2u_n + (u_{n+1} - u_n)^3 + (u_{n-1} - u_n)^3 - \sigma\dot{u}_n + \xi_n(t), \quad (1)$$

where u_n stands for the displacement of the nth unit mass of the chain in dimensionless units ($n = 1, 2 \ldots, N$); σ is the damping parameter (fixed throughout the Letter to $\sigma = 0.04$) and $\xi_n(t)$ is a zero average Gaussian white noise applied independently to each oscillator with the following autocorrelation function:

$$\langle \xi_m(t)\xi_n(0)\rangle = 2D\delta(t)\delta_{mn}. \quad (2)$$

We force the system at the left end as follows:

$$u_0(t) = A\cos(Wt)\cos(\Omega t), \quad (3)$$

while the right boundary condition is free

$$u_N(t) = u_{N+1}(t). \quad (4)$$

As commented below, the value of N should not be too large, in all simulations presented here $N = 6$.

In Fig. 1 we display several characteristic features of stochastic resonance in the FPU chain. Let us first concentrate the attention on the top-right plot, where we show the signal-to-noise ratio (SNR) in decibels. Those who are familiar with stochastic resonance may be surprised to observe multiple peaks in this plot (but see Refs. [18,19]) while, usually, a bell-shaped curve with a single maximum is found. We will explain below this observation, providing an analytical argument based on the continuum limit of the FPU model. The presence of multiple peaks derives from the existence of multiple stable and metastable states for a given forcing amplitute A (the equivalent of having multiple wells in the potential). The forcing signal (3), shown

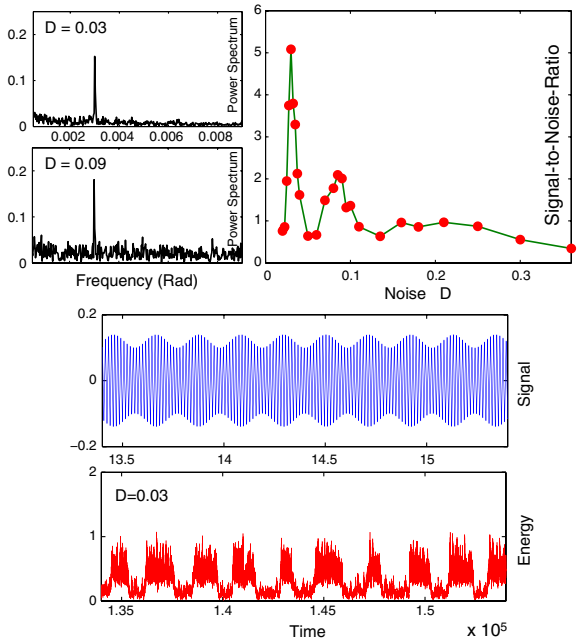

FIG. 1 (color online). Typical signatures of stochastic resonance. In the top-left graph we display the power spectrum of the energy of the FPU chain for the two noise strengths $D = 0.03$ and $D = 0.09$ at which the signal-to-noise ratio (SNR) shows the marked peaks reported in the top-right graph. The forcing signal, with carrier frequency $\Omega = 2.05$ and modulation $W = 0.003$, is plotted in the central graph. The time evolution of the energy for the noise intensity corresponding to the first peak of the SNR plot is shown in the bottom graph: it displays the characteristic bistable features of stochastic resonance.

in the central graph in Fig. 1, has a carrier frequency Ω which is chosen slightly above the upper edge of the linear spectrum $\Omega > \omega_0 = 2$ in order to excite breather type localizations, and is modulated with a much smaller frequency $W \ll \Omega$. This latter frequency plays the role of the forcing frequency appearing in standard stochastic resonance. There is a wide range of values of both A and W for which we can observe stochastic resonance in the FPU model, given that we respect the important condition $\sigma \gg W$. It must be, however, remarked that the amplitude A should be in a range where a stable stationary state of the chain, discussed below, coexists with a metastable one. When this condition is met, we vary the noise strength D until we observe the typical oscillations of the energy of the system shown in the lower graph of Fig. 1. The power Fourier spectrum of the energy signal shows a sharp peak at the driving frequency W when the noise intensity is at resonance (top-left graph in Fig. 1).

We develop below our analytical approach. Let us begin by solving the boundary value problem for the FPU chain in the absence of damping and noise. It is well known that the FPU chain is characterized by the following linear dispersion relation $\omega(k) = \sqrt{2(1 - \cos k)}$, hence the spectrum has band edge frequency $\omega_0 = 2$. In order to derive stationary weakly nonlinear solutions (see, e.g., Ref. [20]) of Eq. (1), we seek for solutions of the following standard form [21,22]:

$$u_n(t) = \frac{(-1)^n}{2}[e^{2it}\phi(n,t) + \text{c.c}], \tag{5}$$

where c.c. denotes the complex conjugated term and $\phi(n,t)$ varies slowly with respect to both its arguments. These solutions should be considered as modulations of upper band edge oscillations. The boundary value problem (3) can be rewritten for $\phi(n,t)$ in the form

$$\phi(0,t) = Ae^{i(\Omega-2)t}, \qquad \phi(N+1/2,t) = 0, \tag{6}$$

where the second condition derives from $\phi(N+1) = -\phi(N)$. Moreover, the condition $\delta\omega = \Omega - 2 \ll 1$ must be satisfied for the function $\phi(n,t)$ to be slowly varying with time.

Substituting then (5) into Eqs. (1), and assuming $\phi(n,t)$ to be a continuous function of its variables, one gets, in the weakly nonlinear limit and neglecting higher order derivatives in n and t, the following nonlinear Schrödinger equation [21,22]:

$$i\frac{\partial\phi}{\partial t} + \frac{1}{4}\frac{\partial^2\phi}{\partial n^2} + 3|\phi|^2\phi = 0. \tag{7}$$

We now assume that the system synchronizes with the boundary (6) and define a new parameter B

$$\phi(n,t) = e^{it\delta\omega}\varphi(n), \qquad B = \frac{\partial\varphi(n)}{\partial n}|_{n=N+1/2} \tag{8}$$

[where $\varphi(n)$ is a real function of n] and, as a result, we get the following relation:

$$\left(\frac{\partial\varphi}{\partial n}\right)^2 = B^2 + 4(\Omega-2)\varphi^2 - 6\varphi^4 \tag{9}$$

and its solution in terms of Jacobi elliptic functions [16,23], which, after substitution into Eqs. (8) and (5), gives the following approximate solution for the relative displacements of the oscillators:

$$u_n = (-1)^n Q\cos(\Omega t)\text{cn}(2\sqrt{\gamma}(N+\tfrac{1}{2}-n) - \mathcal{K}(k), k), \tag{10}$$

where $\mathcal{K}(k)$ is the complete elliptic integral of the first kind with a modulus k and all the constant are defined via the single free parameter B as follows:

$$\gamma^2 = \delta\omega^2 + \frac{3}{2}B^2; \quad Q^2 = \frac{\delta\omega+\gamma}{3}; \quad k^2 = \frac{3B^2}{4\gamma(\gamma-\delta\omega)}. \tag{11}$$

The free parameter B is defined by the condition of adaptation to the boundary (3), leading to the following consistency relation:

$$A = Q\text{cn}(2\sqrt{\gamma}(N+\tfrac{1}{2}) - \mathcal{K}(k), k). \tag{12}$$

From this equation one gets all compatible values of B for a fixed driving amplitude A. It turns out that there are mul-

tiple values of B that solve Eq. (12), which in turn implies the existence of multiple compatible patterns of the type (10), which have correspondingly different energies. In Fig. 2 we display these energies as a function of the driving amplitude A. Three branches of solutions are present. For instance, considering the forcing amplitude $A = 0.09$, five possible energy values are found: among these two are unstable, two are stable, and one is metastable, as described in the caption of Fig. 2. For the type 1 and 2 solutions in Fig. 2, one has an excellent correspondence between the analytical expression (10) and the direct numerical simulations of the FPU chain. For type 3 solutions the approximation is not as good and, besides that, the solution is metastable: in numerical simulations it destabilizes and restabilizes during time evolution. We do not display in Fig. 2 solutions corresponding to higher energies, because the semicontinuuum approximation fails and one should use truncated wave approximations [24].

Summarizing, the system is characterized by several threshold amplitudes. When the driving amplitude exceeds the first threshold A_1, the type 1 stable state jumps into the type 2 stable state. By further increasing the driving up to the second threshold A_2, the transition to the type 3 metastable state occurs. In the presence of damping, when reducing the amplitude of the driving, the system does not remain in the higher energy states. Indeed, a lower threshold amplitude appears, $L = 0.03$, below which the system goes back to the lowest energy stable state. Below, when we consider stochastic resonance, we modulate the driving signal in such a way that its amplitude remains above L and below A_1 (typically $A \in [0.10, 0.14]$), in order to realize stochastic transitions between all states. Furthermore, we note that for a fixed driving amplitude A the stable and metastable states are characterized by sufficiently far separated energies. The presence of these "energy levels" can be monitored by keeping the driving amplitude constant and changing the noise intensity, as shown in Fig. 3. It is clearly seen that for the fixed boundary driving amplitude $A = 0.18$ the transition between type 1 and type 2 stable states occurs at the noise intensity $D = 0.021$, while at $D = 0.055$ the system goes from a type 2 stable state to a type 3 metastable state. One should also observe that the averaged energies of each state well correspond to the ones derived from the approximate analytical solutions (10).

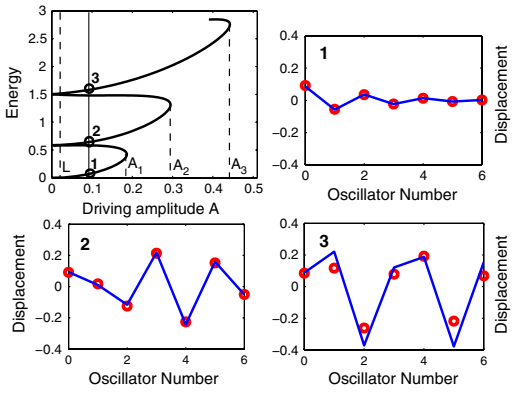

FIG. 2 (color online). In the top-left plot the energy of the approximate solutions (10) of the FPU chain, obtained using our semicontinuum approach is displayed as a function of the driving amplitude A. The intersections of the vertical solid line at $A = 0.09$ with the different branches of the curve correspond to multiple solutions of the consistency relation (12). Type 1 ($E_1 \simeq 0.1$) and 2 ($E_2 \simeq 0.6$) solutions, which turn out to be stable, are compared with numerical simulations (points) in the top-right and bottom-left panels. A type 3 ($E_3 \simeq 1.6$) solution, which is metastable (see text), is represented in the bottom-right panel. $A_1 = 0.18$, $A_2 = 0.31$, and $A_3 = 0.44$ are threshold values for the excitation of the different solutions: A_1 is the driving amplitude for which the transition from a type 1 stationary state to a type 2 stationary state occurs, while A_2 marks the transition from type 2 to type 3 (metastable) solutions, and so on. In the figure, we also display a feature which is present because of the damping and is not taken into account by our approximate solutions: an additional lower threshold L is present (vertical dashed line), below which all the solutions collapse to the type 1 lowest energy state.

Now we are ready to discuss the main result of this Letter. Simulating the FPU model (1) with the driving signal seed frequency $\Omega = 2.05$ and modulating frequency $W = 0.003$, such that the driving signal amplitude A varies in the range $[0.10, 0.14]$, in the presence of both damping and noise, we monitor the time evolution of the system's energy for increasing noise intensities D, and then analyze the properties of its power spectrum $P(\omega)$. The SNR is defined as $\mathrm{SNR} = 10\log_{10}[P(\omega_{\mathrm{peak}})/N(\omega_{\mathrm{peak}})]$, where ω_{peak} is the frequency at which the power spectrum displays a clear peak (see the top-left plots in Fig. 1) and $N(\omega_{\mathrm{peak}})$ is the power of the background noise at the same frequency. For low noise intensities there is no transition between the different states and the system's energy oscillates around E_1. For the noise intensity value $D = 0.03$ (bottom graph in Fig. 1) one observes an oscillation between the state with energy $E_1 = 0.1$ and that with energy $E_2 = 0.6$. Increasing further noise intensity, the SNR drops

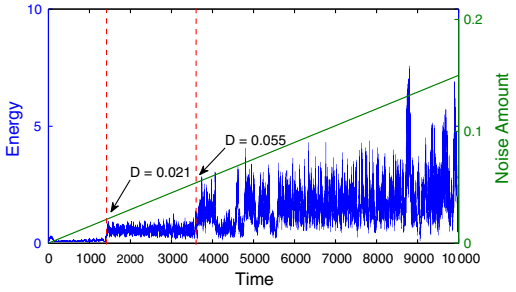

FIG. 3 (color online). Time evolution of the energy of the FPU chain for a constant driving amplitude $A = 0.18$ and a linearly varying noise intensity. Transition from a type 1 to a type 2 state occurs when the noise intensity reaches the threshold value $D = 0.021$, while the transition to a type 3 states takes place at $D = 0.055$. In this simulation, damping is present and the driving is not modulated, $W = 0$.

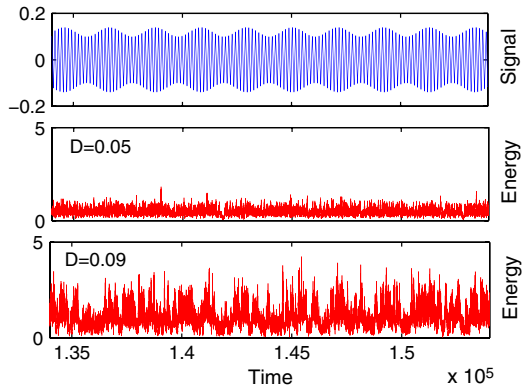

FIG. 4 (color online). Time evolution of the signal (top) and system's energy (central and bottom) at the noise intensities $D = 0.05$ (corresponding to the point between first two peaks of the SNR in Fig. 1) and $D = 0.09$ (second peak of the SNR), respectively.

and the energy fluctuates around the value $E_2 = 0.6$ (middle plot in Fig. 4 for $D = 0.05$). Finally, for the noise intensity $D = 0.09$, which corresponds to the second peak of the SNR in Fig. 1, we observe noisy transitions between the metastable state of energy $E_3 = 1.6$ and two stable states with energies E_1 and E_2 (see the bottom graph of Fig. 4). We do not discuss here the smooth third peak observed in Fig. 1, which is connected to transitions to higher energy states, of which we do not have a clear analytical characterization.

As remarked above, we have performed all our numerical analysis for *short* FPU chains (throughout the Letter $N = 6$), but the observation of this phenomenology is not restricted to this case. Indeed, it should be mentioned that, if in the equations for the β-FPU chain (1) we would have rescaled the strength of the nonlinear coupling by f, the semicontinuum approach developed here gives exactly the same solutions (10), provided that the number of particles N is increased maintaining the ratio $\sqrt{f}/N$ constant.

Concluding, we have considered a damped β-FPU chain forced at one boundary with a modulated signal under the action of an increasing noise level. For specific values of the noise intensity, the power spectrum of the system's energy displays sharp peaks at the modulating frequency. Correspondingly, also the signal-to-noise ratio shows pronounced peaks as a function of noise intensity. This is a clear observation of stochastic resonance in an extended system. Multiple peaks of the SNR are observed, instead of a single broad bump. In order to explain this feature, we have developed a semicontinuum analytical approach, which allows us to point out the presence of multiple stable and metastable solutions for a given forcing amplitude. Stochastic resonance is shown to be generated by transition between these states. These studies could be readily extended to realistic physical systems with local forcing.

R. Kh. acknowledges financial support of the Georgian National Science Foundation (Grant No GNSF/STO7/4-197) and the U.S. Civilian Research and Development Foundation (No. GEP2-2848-TB-06). This work is part of the PRIN07 project Statistical physics of strongly correlated systems at and out of equilibrium: exact results and quantum field theory methods.

[1] R. Benzi, G. Parisi, A. Sutera, and A. Vulpiani, Tellus **34**, 10 (1982); R. Benzi, A. Sutera, and A. Vulpiani, J. Phys. A **14**, L453 (1981).
[2] C. Nicolis, Sol. Phys. **74**, 473 (1981); C. Nicolis and G. Nicolis, Tellus **33**, 225 (1981).
[3] S. Fauve and F. Heslot, Phys. Lett. A **97**, 5 (1983).
[4] B. McNamara and K. Wiesenfeld, Phys. Rev. A **39**, 4854 (1989).
[5] L. Gammaitoni, P. Hanggi, P. Jung, and F. Marchesoni, Rev. Mod. Phys. **70**, 223 (1998).
[6] E. Arimondo and B. M. Dinelli, Opt. Commun. **44**, 277 (1983).
[7] A. Longtin, J. Stat. Phys. **70**, 309 (1993).
[8] E. Fermi, J. Pasta, S. Ulam, and M. Tsingou, in *The Many-Body Problems*, edited by D. C. Mattis (World Scientific, Singapore, 1993); *The Fermi-Pasta-Ulam Problem: A Status Report*, edited by G. Gallavotti (Springer, New York, 2008).
[9] J. Lindner *et al.*, Phys. Rev. Lett. **75**, 3 (1995); M. E. Inchiosa and A. R. Bulsara, Phys. Rev. E **52**, 327 (1995); J. F. Lindner, S. Chandramouli, A. R. Bulsara, M. Locher, and W. L. Ditto, Phys. Rev. Lett. **81**, 5048 (1998).
[10] M. Locher, G. A. Johnson, and E. R. Hunt, Phys. Rev. Lett. **77**, 4698 (1996).
[11] R. Khomeriki and J. Leon, Phys. Rev. E **71**, 056620 (2005).
[12] R. Khomeriki, S. Lepri, and S. Ruffo, Phys. Rev. E **70**, 066626 (2004).
[13] T. Dauxois, R. Khomeriki, F. Piazza, and S. Ruffo, Chaos **15**, 015110 (2005).
[14] O. H. Olsen and M. R. Samuelsen, Phys. Rev. B **34**, 3510 (1986).
[15] D. Chevriaux, R. Khomeriki, and J. Leon, Phys. Rev. B **73**, 214516 (2006).
[16] R. Khomeriki and J. Leon, Phys. Rev. Lett. **94**, 243902 (2005).
[17] R. Khomeriki, J. Leon, and M. Manna, Phys. Rev. B **74**, 094414 (2006).
[18] J. F. Lindner, B. J. Breen, M. E. Wills, A. R. Bulsara, and W. L. Ditto, Phys. Rev. E **63**, 051107 (2001).
[19] X. Luo and Sh. Zhu, Phys. Rev. E **67**, 021104 (2003).
[20] S. Flach and C. R. Willis, Phys. Rep. **295**, 181 (1998).
[21] Yu. A. Kosevich and S. Lepri, Phys. Rev. B **61**, 299 (2000).
[22] R. Khomeriki, Phys. Rev. E **65**, 026605 (2002).
[23] P. F. Byrd and M. D. Friedman, *Handbook of Elliptic Integrals for Engineers and Physicists* (Springer, Berlin, 1954).
[24] Yu. A. Kosevich, Phys. Rev. Lett. **71**, 2058 (1993); Phys. Rev. B **47**, 3138 (1993).